Isolated Semi Integrated On-board Charger for EVs Equipped with 6-phase Traction Drives

Isolated Semi Integrated On-board Charger for EVs Equipped with 6-phase Traction Drives

Paolo Pescetto
Department of Energy "Galileo Ferraris"
Politecnico di Torino
Torino, Italy
paolo.pescetto@polito.it

Gianmario Pellegrino
Department of Energy "Galileo Ferraris"
Politecnico di Torino
Torino, Italy
gianmario.pellegrino@polito.it

***Abstract*—The recent trend in road transportation electrification pushes the development of reliable and compact solutions for the traction drives and charging infrastructures. This work proposes an innovative on-board battery charger partially integrated with the powertrain of a road electric vehicle equipped with a 6-phase traction motor drive. The integration permits to exploit the traction inverter and motor as power conversion unit and HF transformer respectively, with remarkable benefits in terms of e-axle compactness and cost of the components. Despite the integrated nature of the proposed system, galvanic isolation is provided, ensuring reliable and safe operation of the charger. Over to the traction drive, the proposed topology only requires a passive diode bridge and three grid inductors. A dedicated control strategy is developed to avoid torque production during charging. The proposal is validated by exhaustive simulations. A full experimental stage is currently ongoing, and promising preliminary results are reported.**

***Index Terms*—On-board battery charger, Integrated OBC, Traction drives, Multiphase, Multi-three phase drives, PMSM**

I. Introduction

The electrification process in transportation, and especially in road vehicles, has been considerably accelerated by the recent interest from public institutions and private enterprises [1]. This trend is pushing for research and innovation in every component of the Electric Vehicles (EVs), including the development of innovative motor design techniques [2], traction inverters, DC/DC converters, accurate control strategies, batteries and battery chargers [3].

A key technology enabling a vastly spread of EVs is the availability of fast and reliable battery chargers, normally divided into on-board and off-board converters. If the off-board chargers can often reach considerably higher charging power [4], the On-board Battery Chargers (OBC) permit to charge the vehicle battery almost everywhere, thus representing a crucial component of the EV [5]. Common requirements for the OBCs are high efficiency, reliability, compactness and reduced cost of the components.

The OBCs can be divided into stand-alone and integrated solutions [5], as shown in Fig. 1. In the first case, the OBC is a dedicated converter employed at battery charging stage only and optimized for this purpose. On the other side, the integrated chargers (IOBCs) are based on a reconfiguration of the traction drive, which is also involved during charging stage [5]–[7]. In particular, the traction inverter is employed as power conversion unit, while the electrical machine as reactive component. This permits a higher compactness of the e-axle, avoiding an additional converter out of the traction drive, at the cost of a more complicated topology of the EV.

The employment of multiphase machines, and particularly multi-three phase motors, is becoming a standard in high power applications, such as wind turbines, ship propulsion and aerospace [8], [9]. Anyway, thanks to the fast development of multi-three phase technologies in terms of motor and converter design and their control, such drives are progressively extending their usage to lower power applications, including EVs [10], [11]. The adoption of multi-three phase motors in traction drives permits a lower phase current rating, lower torque oscillation, improved reliability in case of failure and advantages on the cooling circuit [12], [13].

A common drawback of most of the integrated OBCs, designed for 3-phase drives [6], [7], is that the galvanic isolation between the main inlet and the traction battery is not provided. This can cause safety issues and common mode capacitive currents [14]. Very few examples of isolated chargers integrated with EVs traction drives are found in literature. In [15], a wound field Induction Motor (IM) is

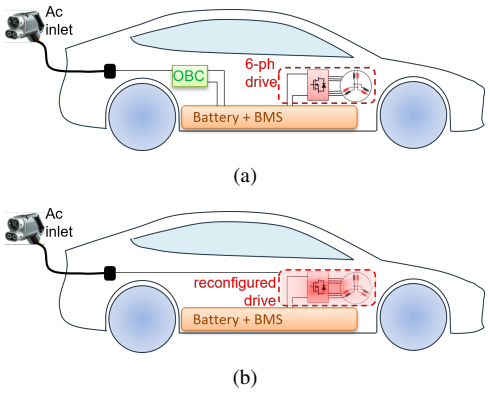

Fig. 1. On-board charger an EV. (a) Stand-alone and (b) integrated OBC.

The authors are grateful to the European Commission for the support to the present work, performed within the EU H2020 project FITGEN (Grant Agreement 824335).

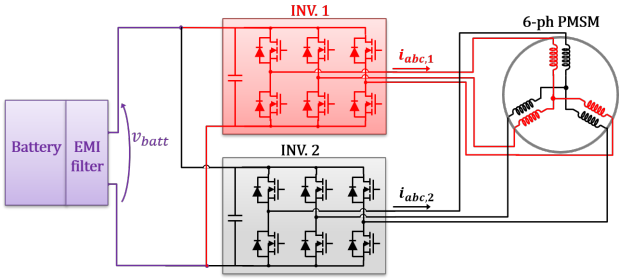

Fig. 2. Topology of the considered EV in traction mode.

TABLE I
RATINGS OF THE TRACTION DRIVE.

motor		
rated power	96	kW
rated torque	220	Nm
base speed	5100	rpm
max speed	12000	rpm
pole pairs	3	
6-phase inverter		
phase current	115	Arms
DC voltage	400	V
switching frequency	12÷50	kHz

adopted, and the grid inlet is connected to the stator terminals at charging stage. This solution effectively isolates the battery from the grid, but wound field IMs are rarely adopted in EVs because of their complex manufacturing and need of rotating contacts, which ultimately require additional maintenance.

The integration of a charger with a multiphase drive [16]–[18] permits additional degrees of freedom in the e-axle reconfiguration and control. In particular, the solutions in [16] exploit a dedicated reconfiguration of the multiphase machine to use it as a boost inductor, but without providing galvanic isolation between the battery and the grid. Galvanic isolation is claimed in [17], but assuming an off-board isolating transformer, so it is not achieved by the OBC itself. This is obtained by the Isolated Fully-Integrated charger (IFI-OBC) proposed in [18], where a 6-phase machine is used as isolation transformer, thus electrically separating the two sides without any additional electrical hardware respect to the traction drive itself. Anyway, the e-motor was excited at grid voltage amplitude and frequency, thus requiring a reconfiguration of the motor windings to increase the number of turns to avoid excessive core saturation, which may be a relevant mechanical challenge.

This work proposes an innovative solution, named **Isolated Semi-Integrated On-Board Charger (ISI-OBC)** [19] for integrating a battery charger with a 6-phase traction motor drive, exploited as isolation transformer. Differently from [18], the motor excitation frequency is inverter controlled to be compatible with the machine ratings, thus not requiring windings reconfiguration, which is a major advantage respect to the ISI-OBC topology. The required additional components are limited to a simple 3-phase diode bridge and three input inductors. Moreover, the proposed charger is compatible with single- and three-phase main inlet.

II. Vehicle and Charger Ratings

Table I reports the parameters of the drive under test, designed for an A-segment EV [10]. The correspondent vehicle architecture is reported in Fig. 2, referring to the traction configuration. As can be seen, the vehicle is motored by a 6-phase internal NdFeB PM Synchronous Machine (PMSM). The stator phases are grouped into two symmetric three-phase sets [12], [13], [20], labeled with the subscripts 1 and 2. Each set is fed by an automotive 2-levels 3-phase inverter designed for 400 V DC-link, called INV.1 and INV.2. Thanks to the symmetry of the two sets, the proposed solution can be identically applied reverting the sets 1 and 2.

In this work, a commercial 3-phase traction motor [21] has been re-wounded in a symmetrical 6-phase configuration, maintaining the same number of turns of each set. Therefore, each 3-phase winding set of the modified motor presents the same rated voltage, but half the rated current respect to [21], thus maintaining the same saturation characteristic. For this machine, the torque is roughly equally split between PM and reluctance contributions.

The flux maps of the 6-phase motor are depicted in Fig. 3. It is designed for medium-high speed (12000 rpm), as common for modern EVs. As a consequence, the inductance is only few mH and the core saturates at ≈0.1 Vs.

The considered application [10] and standards [22] impose the specifications for the IOBC. First, the safety standards impose that the EV battery must be galvanically isolated from the grid during charging. Additionally, the deepest possible integration with the drive is pursued, thus limiting eventual additional hardware components out of the traction configuration. The charger should be compatible with both single- and three-phase main inlet, to increase its flexibility, and capable of charging the battery either in Constant Voltage (CV) or Constant Current (CC) modes. Dealing with the motor, shaft torque or movement and windings overheating must be avoided during charging. Finally, the standards require a grid current THD $< 5\%$ with a PF>0.95.

III. Modeling of the 6-phase Machine

This section describes the equations modeling the dual 3-phase PMSM. **Bold** symbols define vector quantities. The subscripts 1 and 2 refer to the two 3-phase sets, while the quantities without subscript number refer to magnetizing components. The direction of PM magnetization defines the rotor d axis. Fig. 2 reports the six currents definition.

The voltage in each 3-phase set $\boldsymbol{v_{dq,1}}$ and $\boldsymbol{v_{dq,2}}$ can be conveniently expressed in the rotating dq reference frame:

$$\begin{cases} \boldsymbol{v_{dq,1}} = R_s \boldsymbol{i_{dq,1}} + \frac{\mathrm{d}\boldsymbol{\lambda_{dq,1}}}{\mathrm{d}t} + \mathbf{J}\omega\boldsymbol{\lambda_{dq,1}} \\ \boldsymbol{v_{dq,2}} = R_s \boldsymbol{i_{dq,2}} + \frac{\mathrm{d}\boldsymbol{\lambda_{dq,2}}}{\mathrm{d}t} + \mathbf{J}\omega\boldsymbol{\lambda_{dq,2}} \end{cases} \quad (1)$$

being R_s the stator resistance, ω the electrical angular frequency and $\mathbf{J} = \begin{bmatrix} 0 & -1 \\ 1 & 0 \end{bmatrix}$ the complex operator matrix. Because of the inherent magnetic coupling of the two 3-phase

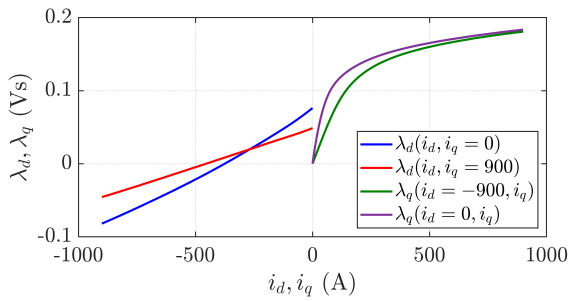

Fig. 3. Saturation flux maps of the motor under test.

sets, each flux linkage depends on each of the 6 currents. Moreover, the current-to-flux characteristic is highly non-linear due to core saturation effects:

$$\begin{cases} \boldsymbol{\lambda_{dq,1}} = \boldsymbol{\lambda_{dq,1}}\left(\boldsymbol{i_{dq,1}}, \boldsymbol{i_{dq,2}}\right) \\ \boldsymbol{\lambda_{dq,2}} = \boldsymbol{\lambda_{dq,2}}\left(\boldsymbol{i_{dq,1}}, \boldsymbol{i_{dq,2}}\right) \end{cases} \tag{2}$$

The magnetizing current $\boldsymbol{i_{dq}}$ is defined as:

$$\boldsymbol{i_{dq}} = \boldsymbol{i_{dq,1}} + \boldsymbol{i_{dq,2}} \tag{3}$$

Similarly to a transformer, the flux linkage in each 3-phase set is given by a magnetizing component plus a leakage term:

$$\begin{cases} \boldsymbol{\lambda_{dq,1}} = \boldsymbol{\lambda_{dq}} + L_\sigma \boldsymbol{i_{dq,1}} \\ \boldsymbol{\lambda_{dq,2}} = \boldsymbol{\lambda_{dq}} + L_\sigma \boldsymbol{i_{dq,2}} \end{cases} \tag{4}$$

where L_σ is the leakage inductance. The magnetizing flux is retrieved from the common mode flux and current:

$$\boldsymbol{\lambda_{dq}} = \frac{\boldsymbol{\lambda_{dq,1}} + \boldsymbol{\lambda_{dq,2}}}{2} - L_\sigma \frac{\boldsymbol{i_{dq,1}} + \boldsymbol{i_{dq,2}}}{2} \tag{5}$$

The relationship between $\boldsymbol{i_{dq}}$ and $\boldsymbol{\lambda_{dq}}$ corresponds to the saturation characteristic of the original 3-phase machine [21] and is defined by the flux maps in Fig. 3, measurable as in [23]. Finally, the motor torque can be computed as:

$$T = \frac{3}{2} p \left(\lambda_d i_q - \lambda_q i_d\right) \tag{6}$$

IV. Proposed Isolated Semi-Integrated Charger

The proposed ISI-OBC topology is reported in Fig. 4 [19]. The base idea is to exploit the 6-phase PMSM during charging as an HF transformer, isolating the battery from the grid inlet. Differently from the IFI-OBC in [**?**], [18], the excitation frequency is arbitrarily imposed by the converter to be compatible with the ratings of the machine, thus not requiring modifications in the stator windings.

In charging mode, the two inverter units still share the same DC-link, but this is separated from the battery. One of the two inverters (INV.2) is disconnected from its winding set and connected to the grid by means of dedicated inductors. Meanwhile, INV.1 properly excites the PMSM, regulating the power transfer to the battery without torque production. The induced EMF on the second 3-phase set of the PMSM, i.e. the secondary side of the equivalent transformer, is rectified by a 3-phase diode bridge, charging the battery.

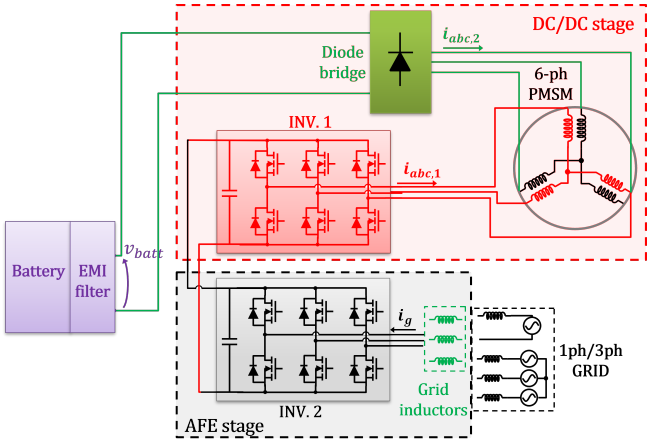

Fig. 4. Proposed Isolated Semi-Integrated configuration. The additional components respect to the traction drive are highlighted in green.

The additional components respect to the base traction drive in Fig. 2 are limited to the input inductors and a passive 3-phase diode bridge. If compared with a traditional stand-alone OBC, similar input inductors are needed but most of the other components are saved, including dedicated HF transformer, power modules, drivers and bus capacitors. Another the benefit of the ISI-OBC is that the electrical power required at charging stage (up to 11 kW) is considerably lower than the rated power of the motor (96 kW). Therefore, the electrical machine is operating with an RMS phase current much lower than during traction, and consequently reduced Joule losses. Otherwise said, despite the application required an 11 kW OBC a considerably larger power could be achieved.

A. Grid Interface

The module INV.2 is adopted for rectifying the grid voltage (gray box in Fig. 4). Similarly to a standard Active Front-End (AFE) rectifier, the purpose of this converter is to guarantee sinusoidal grid current with unitary PF, and to provide a stable DC-link to supply the INV.1 unit. The grid connection requires dedicated input inductors to control the grid current. The number and size of such inductors depend on the required OBC power level and grid inlet. Some examples include:

- in case the of 3-phase main inlet, three input inductors are required, and the INV.2 module can be controlled as 3-phase AFE rectifier.
- With single-phase inlet, a single grid inductor can be employed, with the grid connected to two legs of INV.2, forming an H-bridge.
- Alternatively, still for single-phase inlet the three legs of INV.2 can be exploited in interleaving configuration, using 3 grid inductors.

All listed options correspond to well-established topologies of grid connected converters [5], so standard algorithms can be employed to control the grid current waveform and PF. It should be noted that the INV.2 is a 3-phase inverter for automotive traction, so its phase current ratings (115 Arms) and switching frequency (12÷50 kHz) are widely larger respect to the minimum required for operating as AFE. Overall, the grid interface is not critical, and several degrees of freedom

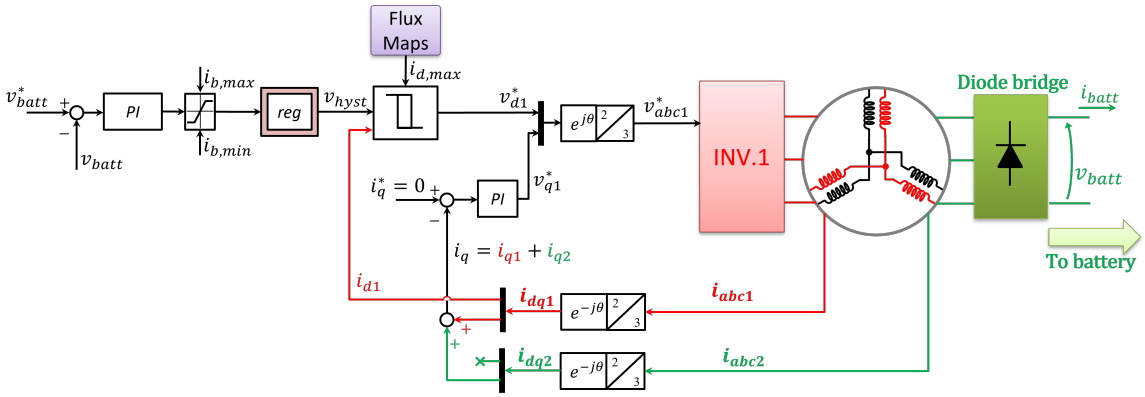

Fig. 5. Block scheme of the proposed charging control strategy.

are left for the designers in terms of topologies, sizing of the components and control strategies. For this reason, this work will focus on the proposed DC/DC conversion stage.

B. Isolated DC/DC Stage

The core of the proposed topology is using the traction drive as an HF isolation transformer in the DC/DC charger stage (red box in Fig. 4). The connection of INV.1 to its winding set is not modified respect to the traction configuration. This inverter unit is employed to excite the machine. The controlled excitation of the PMSM permits to regulate its frequency to be compatible with the rated value during traction, to avoid excessive core saturation and torque production and to regulate the battery current. Thanks to the magnetic coupling between the two 3-phase winding sets (2), a relevant EMF at the excitation frequency will be induced in the second set, connected to the diode bridge.

V. Control Strategy

As mentioned, the INV.2 is configured in standard AFE topologies and the related known control techniques can be adopted. Therefore, the control of the AFE stage will not be discussed here. On the other hand, the control of INV.1 is not trivial. It should be noted that, despite the flux and current response depends on both the 3-phase sets, only the voltage on the first set can be controlled. The block diagram of the proposed algorithm, operating in rotor dq coordinates, is reported in Fig. 5. The d axis is devoted to the machine excitation and battery charging control, whereas the q axis control actively forces zero shaft torque.

The reference voltage in d axis v^*_{d1} is a bipolar square wave with constant amplitude v_{hyst}, which sign is reversed every time the measured current i_{d1} overcomes a defined threshold value $i_{d,max}$, in an hysteresis mechanism. The charging power is regulated by acting on the amplitude of v_{hyst}. The relationship between v_{hyst} and the obtained battery current i_{batt} is non-linear, and currently under investigation. Similarly to stand-alone OBCs, the reference battery current i^*_{batt} is determined by an external battery voltage loop and limited between its minimum and maximum values $i_{b,min}$ and $i_{b,max}$, thus permitting both CC and CV operating mode.

The amplitude of $i_{d,max}$ is determined based on the machine flux maps in Fig. 3 in order to avoid excessive core saturation. Additionally, $i_{d,max}$ can be adjusted if needed to set the reversal frequency of the square wave hysteresis voltage, i.e. the excitation frequency of the equivalent transformer.

The q axis is regulated by a closed loop current control, with the goal of avoiding shaft torque at charging stage. The feedback of the current loop is the magnetizing current i_q, given by the sum between i_{q1} and i_{q2} (3), while the reference is zero. By forcing $i_q = 0$ the machine is excited along the d axis, i.e. in the direction of the PM, so the torque is null (6). The calibration of this PI regulator can be easily done based on the machine flux maps (Fig. 3).

It should be noted that the control strategy depicted in Fig. 5 effectively limits the phase current within the desired values, thus without considerably heating the motor. Moreover, it is independent by the rotor position, which is commonly random at charging stage, so it does not require any initial alignment or rotor movement. Finally, it can be remarked that the flux maps are normally required for an accurate motor control during traction, so their employment at charging stage does not add particular issue to the control calibration.

VI. Validation

The proposed ISI-OBC topology and control strategy was deeply validated in simulation. A complete experimental stage is currently ongoing, with promising results.

A. Simulation Results

The proposed system was simulated in PLECS environment using an accurate model of the 6-phase machine and the power electronic converters. As detailed in Section IV-A, the exploitation of INV.2 as an active front end is open to several possibilities for the designers, but standard topologies and control strategies can be adopted. Therefore, the results related to the AC/DC conversion stage are not reported here.

On the other hand, the simulation results deeply focus on the DC/DC stage, demonstrating the effective capability of the machine to work as an HF isolation transformer. The control strategy detailed in Section V was adopted, thus controlling i_{d1} based on an hysteresis mechanism, while $i_q = 0$ was

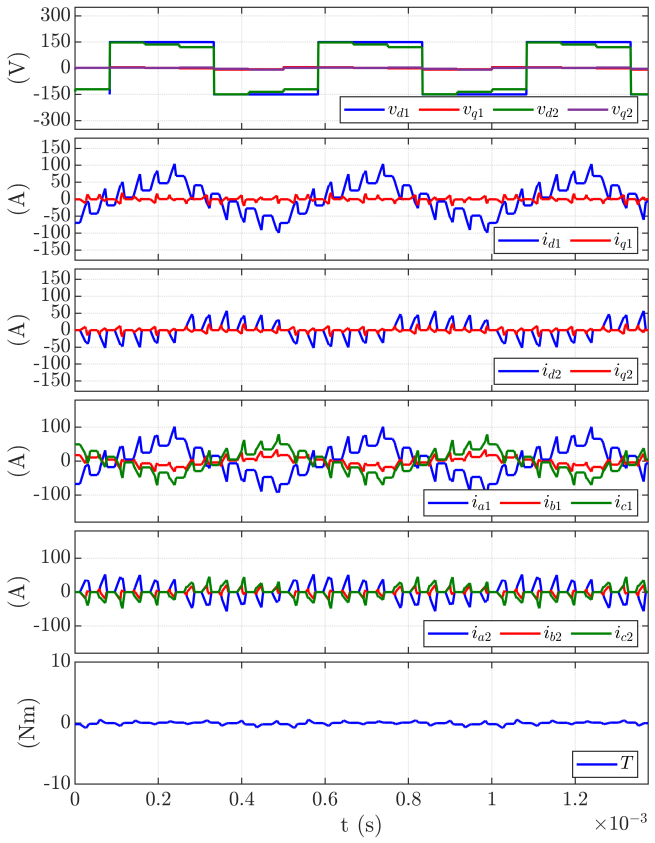

Fig. 6. Simulation results for a charging power of 5.5 kW (V_{hyst}=150 V).

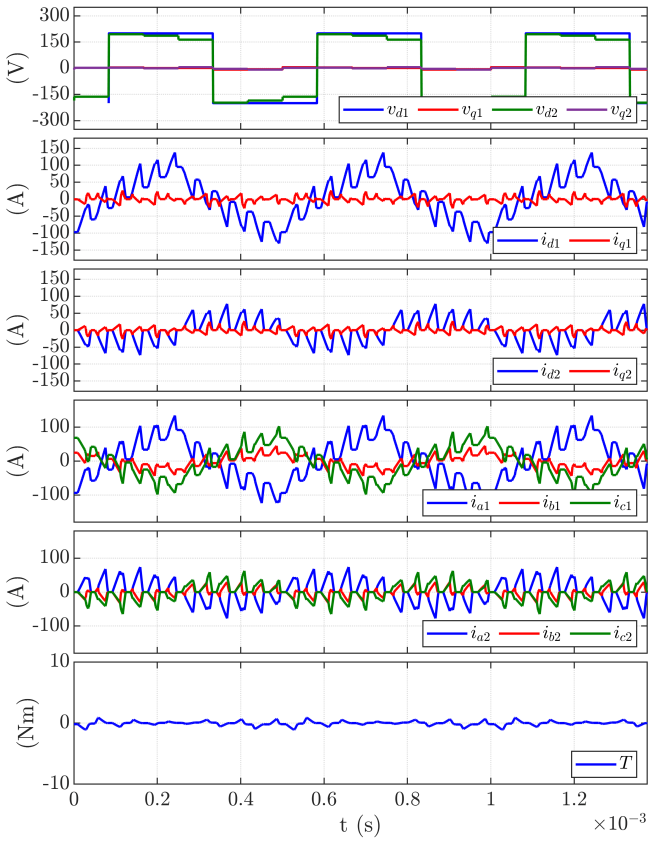

Fig. 7. Simulation results for a charging power of 10 kW (V_{hyst}=200 V).

forced through a closed loop current control. The converter INV.1 is simulated at its minimum switching frequency ($f_{sw} = 12\ kHz$, see Table I). It is worth noticing that a more accurate control can be obtained with a higher switching frequency.

Two examples of results are depicted in Fig.s 6 and 7, for a charging power of 5.5 kW and 10 kW respectively. Both cases were simulated with a threshold $i_{d,max} = 60\ A$, which does not saturate the machine. Due to the low ratio between f_{sw} and the hysteresis frequency, the current presents a significant overshoot respect to $i_{d,max}$, whose entity can be easily predicted and compensated knowing the machine inductance and the applied v_{hyst}. The regulation of the charging power was obtained by varying the amplitude of the v_{hyst}, imposed at 150 V and 200 V in the two cases.

As can be seen in the first subplot of the two Figures, thanks to the good coupling between the two 3-phase sets the voltage in the second set $\boldsymbol{v_{dq,2}}$ resembles $\boldsymbol{v_{dq,1}}$, except for a limited voltage drop due to the stator resistance and the leakage flux. The current control is also working well, with i_{d1} correctly limited by the hysteresis mechanism (see the second subplot) and the magnetizing $i_q = i_{q1} + i_{q2}$ is reasonably null. The phase currents in the two sets of windings are reported in the fourth and fifth subplots. It can be noted that the current in the second 3-phase set is pulsating. This is explained considering that the secondary side is connected to a diode bridge, and each diode is not polarized for the entire PWM period. The last subplot depicts the shaft torque, which is approximately zero, with oscillations bounded between ± 1 Nm at the PWM frequency. Finally, Fig. 8 depicts the battery voltage and current. The v_{batt} is well stable, while i_{batt} presents an oscillation at twice the hysteresis frequency due to the single phase nature of the machine excitation. This oscillation can be damped by the EMC filter, normally present in traction batteries.

B. Preliminary Experimental Results

As mentioned in Section II, the present study is based on the commercial motor [21], rewounded in a 6-phase configuration maintaining the same voltage rating and half current capability per each 3-phase set. Fig. 9 depicts the test bench and the 6-phase machine, in the right side of the picture. As can be noted, the proposed ISI-OBC is tested at free-shaft, which is

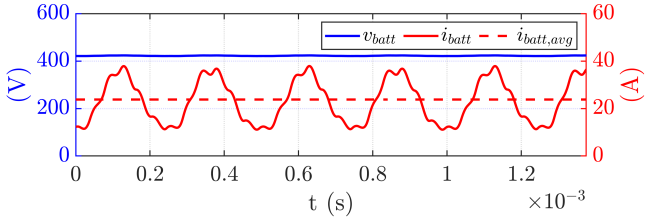

Fig. 8. Battery voltage an current for a charging power of 10 kW.

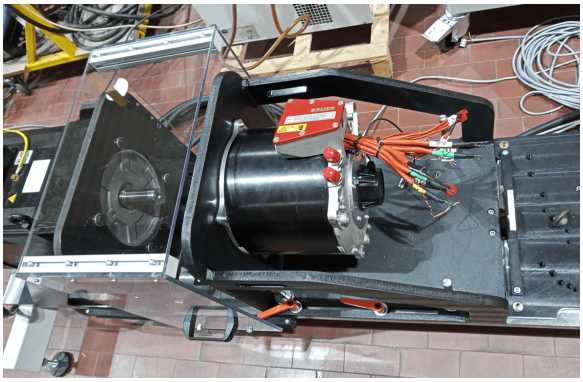

Fig. 9. Picture of the 6-phase machine on the experimental test bench.

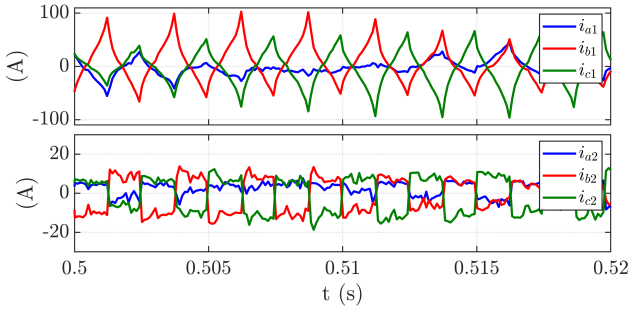

Fig. 10. Preliminary experimental results for a charging power of 5 kW.

the most challenging condition for avoiding rotor movement during charging, as the dyno drive in the other side of the bench is mechanically disconnected from the motor under test. The preliminary experimental results, are promising and in accordance with the simulations. An example is given in Fig. 10, showing the currents in the first and second 3-phase set for a charging power of 5 kW.

VII. Conclusions

This paper proposes a novel solution for an OBC integrated with a 6-phase traction drive. Galvanic isolation between the grid and the battery is obtained by exploiting the PMSM as a HF transformer. The required additional hardware is limited to a passive diode bridge and one to three input inductors. This merges the compact nature of the integrated chargers with the safety requirements imposed by the automotive standards. A dedicated control strategy is developed, which permits to regulate the flux excitation frequency and amplitude, to properly exploit the magnetic coupling between the two 3-phase sets, without shaft torque production and without requiring any rotor movement, independently by the rotor position. Accurate simulation results and preliminary experiments demonstrate the feasibility of the proposed solution; a full experimental validation is currently ongoing.

Acknowledgment

The authors are grateful to the European Commission for the support to the present work, performed within the EU H2020 project FITGEN (Grant Agreement 824335).

The research has been conducted with the support of Power Electronics Innovation Center (PEIC) of Politecnico di Torino.

References

[1] IEA, “Global EV Outlook 2020,” 2020. [Online]: https://www.iea.org/reports/global-ev-outlook-2020. [Accessed June 23rd 2021].

[2] R. Leuzzi et Al., ”Transient Overload Characteristics of PM-Assisted Synchronous Reluctance Machines, Including Sensorless Control Feasibility,” in *IEEE Transactions on Industry Applications*, vol. 55, no. 3, May-June 2019.

[3] A. Krings and C. Monissen, ”Review and Trends in Electric Traction Motors for Battery Electric and Hybrid Vehicles,” *2020 International Conference on Electrical Machines (ICEM)*, Gothenburg, Sweden, 2020.

[4] H. Tu, H. Feng, S. Srdic and S. Lukic, ”Extreme Fast Charging of Electric Vehicles: A Technology Overview,” in IEEE Transactions on Transportation Electrification, vol. 5, no. 4, pp. 861-878, Dec. 2019.

[5] M. Yilmaz and P. T. Krein, ”Review of Battery Charger Topologies, Charging Power Levels, and Infrastructure for Plug-In Electric and Hybrid Vehicles,” in *IEEE Transactions on Power Electronics*, 2013.

[6] L. Solero, ”Nonconventional on-board charger for electric vehicle propulsion batteries,” in *IEEE Transactions on Vehicular Technology*, vol. 50, no. 1, pp. 144-149, Jan. 2001.

[7] US Patent US8847555B2, ”Fast charging device for an electric vehicle”.

[8] E. Levi, ”Multiphase Electric Machines for Variable-Speed Applications,” in *IEEE Transactions on Industrial Electronics*, 2008.

[9] S. Rubino et Al. ”Vector Control of Multiple Three-Phase Permanent Magnet Motor Drives,” *IECON 2018 - 44th Annual Conference of the IEEE Industrial Electronics Society*, 2018.

[10] M. Martino, P. Pescetto and G. Pellegrino, ”Advanced Functionally Integrated E-Axle for A-Segment Electric Vehicles,” 2020 AEIT International Conference of Electrical and Electronic Technologies for Automotive (AEIT AUTOMOTIVE), Turin, Italy, 2020, pp. 1-6.

[11] A. Salem and M. Narimani, ”A Review on Multiphase Drives for Automotive Traction Applications,” in IEEE Transactions on Transportation Electrification, vol. 5, no. 4, pp. 1329-1348, Dec. 2019.

[12] F. Barrero and M. J. Duran, ”Recent Advances in the Design, Modeling, and Control of Multiphase Machines—Part I,” in *IEEE Transactions on Industrial Electronics*, Jan. 2016.

[13] P. Pescetto, S. Ferrari, G. Pellegrino, E. Carpaneto and A. Boglietti, ”Winding Thermal Modeling and Parameters Identification for Multi-three Phase Machines Based on Short-Time Transient Tests,” in *IEEE Transactions on Industry Applications*, vol. 56, no. 3, 2020.

[14] M. Valente et Al., ”Integrated On-Board EV Battery Chargers: New Perspectives and Challenges for Safety Improvement,” *2021 IEEE Workshop on Electrical Machines Design, Control and Diagnosis (WEMDCD)*, Modena, Italy, 2021.

[15] F. Lacressonniere et al., “Converter used as a battery charger and a motor speed controller in an industrial truck,” in *2005 European Conference on Power Electronics and Applications,* 7 pp.-P.7 2005.

[16] I. Subotic, N. Bodo, E. Levi, B. Dumnic, D. Milicevic and V. Katic, ”Overview of fast on-board integrated battery chargers for electric vehicles based on multiphase machines and power electronics,” in *IET Electric Power Applications*, vol. 10, no. 3, pp. 217-229, 3 2016.

[17] I. Subotic, N. Bodo, E. Levi, M. Jones and V. Levi, ”Isolated Chargers for EVs Incorporating Six-Phase Machines,” in *IEEE Transactions on Industrial Electronics*, vol. 63, no. 1, pp. 653-664, Jan. 2016.

[18] P. Pescetto and G. Pellegrino, ”Integrated Isolated OBC for EVs with 6-phase Traction Motor Drives,” *2020 IEEE Energy Conversion Congress and Exposition (ECCE)*, Detroit, MI, USA, 2020.

[19] P. Pescetto and G. Pellegrino, *”Isolated semi-integrated on-board battery charger (ISI-OBC) for electric vehicles”*, Italian patent pending 102021000011036, April 30, 2021. [Online]: https://www.knowledge-share.eu/brevetto/caricabatteria-di-bordo-semi-integrato-per-veicoli-elettrici/

[20] P. Xu et Al., ”Analysis of Dual Three-Phase Permanent-Magnet Synchronous Machines With Different Angle Displacements,” in *IEEE Transactions on Industrial Electronics*, vol. 65, no. 3, 2018.

[21] Brusa Elektronik, HSM1-6.17.12 traction motor. https://www.brusa.biz/portfolio/hsm1-6-17-12/?lang=en [Accessed June 23rd 2021]

[22] International standard IEC 61851-21-1:2017 - Electric vehicle conductive charging system - Part 21-1 Electric vehicle on-board charger EMC requirements for conductive connection to AC/DC supply.

[23] P. Pescetto and G. Pellegrino, ”Sensorless magnetic model and pm flux identification of synchronous drives at standstill,” *2017 IEEE International Symposium on Sensorless Control for Electrical Drives (SLED)*, Catania, Italy, 2017, pp. 79-84.